

Restricted and unrestricted Hartree-Fock calculations of conductance for a quantum point contact

O. P. Sushkov

School of Physics, University of New South Wales,
Sydney 2052, Australia

Very short quantum wires (quantum contacts) exhibit a conductance structure at a value of conductance close to $0.7 \cdot 2e^2/h$. It is believed that the structure arises due to the electron-electron interaction, and it is also related to electron spin. However details of the mechanism of the structure are not quite clear. Previously we approached the problem within the restricted Hartree-Fock approximation. This calculation demonstrated a structure similar to that observed experimentally. In the present work we perform restricted and unrestricted Hartree-Fock calculations to analyze the validity of the approximations. We also consider dependence of the effect on the electron density in leads. The unrestricted Hartree-Fock method allows us to analyze trapping of the single electron within the contact. Such trapping would result in the Kondo model for the $\backslash 0.7$ structure". The present calculation confirms the spin-dependent bound state picture and does not confirm the Kondo model scenario.

PACS: 73.61.-r, 73.23.Ad, 71.45.Lr

The quantized conductance $G = nG_2$, $n = 1; 2; 3; \dots$, $G_2 = 2e^2/h$, through a narrow quantum point contact was discovered in 1988^{1,2}. This quantization can be understood within a one-dimensional (1D) non-interacting electron gas picture, see e.g. Ref.³. In the present work we are interested in a deviation from the integer quantization. This deviation, the so called $\backslash 0.7$ structure" has been found in experimental works^{4,5}. The structure is a shoulder-like feature or a narrow plateau at $G \approx 0.7G_2$. More recent work demonstrates that there are some above barrier excitations related to the structure⁶, and that the structure evolves down to $G \approx 0.5G_2$ in longer quantum contacts⁷. Dependence of the structure on the longitudinal magnetic field has been studied already in the pioneering work⁴. This study clearly demonstrated that the effect is somehow related to the electron spin. Authors of a recent experimental work⁸ argue that the structure signals formation of a Kondo-like correlated spin state.

There have been suggestions to explain the $\backslash 0.7$ structure" by spontaneous magnetization of the 1D quantum wire^{9,13}, or by formation of a two-electron bound state with nonzero total spin^{14,15}. These suggestions implicitly assume that 2D leads connected to the contact are qualitatively important for the effect because there is the rigorous Lieb-Mattis theorem¹⁶ that claims that the ground state of a 1D many-body system has zero spin.

A Hartree-Fock calculation of the conductance has been performed in the Ref.¹⁷. This calculation demonstrated a structure similar to that observed experimentally. The ground state has zero spin in accordance with the Lieb-Mattis theorem, but nevertheless the structure found in the calculation is intrinsically related to the spin because it disappears without account of the exchange electron-electron Coulomb interaction. The structure is related to the formation of the charge density wave within the contact or in other words to the spin-dependent bound state within the contact.

The present work has been stimulated by the recent suggestion that the $\backslash 0.7$ -structure signals formation of a Kondo-like correlated spin state⁸, see also Ref.¹⁸. The restricted Hartree-Fock (RHF) approximation employed in Ref.¹⁷ is not sufficient to follow this suggestion. However the unrestricted Hartree-Fock (UHF) approach can shed light on the problem. In the present work we consider only zero temperature case. The RHF method implies that spin up and spin down single electron orbitals are identical while in the UHF method those orbitals are completely independent. The RHF is explicitly rotationally invariant, but it is not very effective in accounting for electron-electron correlations. The UHF is much better at accounting for the correlations, but it violates the rotational invariance. There is no doubt that even UHF cannot account for the long range Kondo-like dynamics. However it can indicate localization of a single electron within the contact. This would immediately imply the Kondo-like dynamics. Our calculation shows that such localization can take place in longer contacts and at low electron density in leads. However it always leads to a very special dependence of conductance on the gate voltage which is different from that observed experimentally. In the regime when the dependence of conductance on the gate voltage is similar to the experimental one the results of RHF and UHF are practically identical and this indicates the validity of both approximations. We also study dependence of the $\backslash 0.7$ structure" on the electron density in the leads. The structure disappears at high density and it is getting more pronounced at the low density in a qualitative agreement with experiment.

It is well known, see Ref.³, that in the independent particle approximation, i.e. in the case of an ideal electron gas, the conductance for a given transverse channel is proportional to the barrier transmission probability at Fermi energy T ,

$$G = \frac{2e^2}{h} T; \quad (1)$$

In case of interacting particles this formula should be also valid because before and after the potential barrier

the density of electrons is high enough, and hence the interaction is negligible. However one cannot use a single particle description to calculate the transmission probability T because in the vicinity of the barrier the electron density is low, and hence the many-body effects are very important. To calculate the transmission probability T the following method is applied. Consider electrons on a 1D ring of the length L with a potential barrier of the length l somewhere on the ring. It is important that $L \gg l$. There is no current in the ground state of the system. Now let us apply a magnetic flux through the ring. This flux induces the electric current. Note that it is not a real magnetic field, this is a fictitious gauge field that generates the current without applying any voltage. It is especially convenient to take the gauge field that provides the Bohm-Aharonov phase $\phi = 2\pi$. We use this choice in our calculations. The induced current can be calculated by solving many-body Schrodinger equation. It can be an exact solution or an approximate one like RHF or UHF. It has been demonstrated in Ref.¹⁷ that to find the barrier transmission probability at Fermi energy one has to solve the many-body problem twice: without the barrier and with the barrier. The ratio of electric currents squared gives the transmission probability, $T = (J_U = J_0)^2$. This formula is valid without an external magnetic field. Repeating considerations of Ref.¹⁷ one can prove that with the magnetic field, i.e. with the spin splitting, the effective transmission probability is given by

$$T = \frac{1}{2}T_{\uparrow} + \frac{1}{2}T_{\downarrow}; \quad T = \frac{J_U}{J_0}^2; \quad (2)$$

where $J_{\uparrow/\downarrow}$ is the electric current of electrons with spin up and spin down correspondingly. Equation (2) can be also applied for UHF calculations without an external magnetic field. The relation $T = (J_U = J_0)^2$ has been applied recently to study conductance through a system of strongly correlated spinless fermions¹⁹. In this work the many-body problem has been treated exactly via the Density Matrix Renormalization Group algorithm.

The Hamiltonian of the many body system we consider is of the form

$$H = \sum_i \frac{(p_i - A)^2}{2} + U(x_i) + \frac{1}{2} \sum_{i,j} V(x_i; x_j); \quad (3)$$

where indexes i and j enumerate electrons, x_i is the periodic coordinate on the ring of length L ($0 < x < L$), and $A = \phi/2L$ is the fictitious gauge field. The electron-electron Coulomb repulsion is of the form

$$V(x; y) = \frac{1}{a_t^2 + D^2(x; y)}; \quad (4)$$

where $a_t \approx 2$ is the effective width of the transverse channel, see Ref.¹⁷, and $D(x; y)$ is the length of the shortest arc between the points x and y on the ring. We use atomic units, so distances are measured in units of Bohr radius, $a_B = \hbar^2/m_e e^2$, and energies are measured in units of $E_{unit} = m_e e^4/\hbar^2$, where m is the effective electron mass and ϵ is the dielectric constant. For experimental conditions of works^{4,8} these values are the following: $a_B \approx 10^2$ m, $E_{unit} \approx 10^2$ eV. To model the gate potential we use the following formula for the potential barrier

$$U(x) = \frac{U_0}{e^{(x-jl/2)/d} + 1}; \quad d = l/10; \quad (5)$$

Plots of $U(x)$ for $l=8,10,12$ are shown in Fig.1.

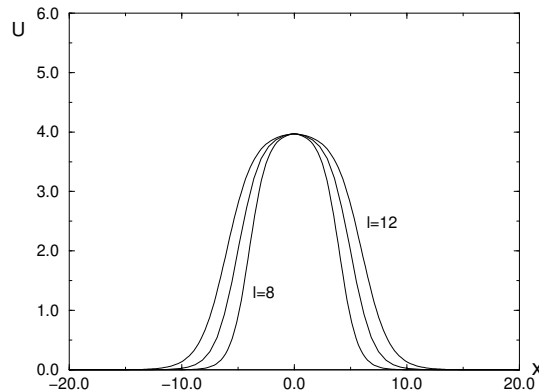


FIG. 1. The "gate" potential (5) at $U_0 = 4$ and $l = 8; 10; 12$.

To solve the many-body problem described by the Hamiltonian (3) we use the Hartree-Fock (HF) approximation. In the HF approximation the many body wave function is represented in the form of the Slater determinant of single particle orbitals $\phi_i(\mathbf{x})$. The index i shows the coordinate state of the orbital, and the index $\sigma = 1, 2$ shows the spin state of the orbital. Each orbital obeys the equation

$$\hat{h}\phi_i = \epsilon_i \phi_i; \quad (6)$$

where ϵ_i is the single particle energy and \hat{h} is the HF Hamiltonian

$$\begin{aligned} \hat{h}\phi_i(\mathbf{x}) &= -\frac{\hbar^2 \nabla^2}{2m} \phi_i(\mathbf{x}) + U_{\text{eff}}(\mathbf{x}) \phi_i(\mathbf{x}) + \sum_j \int d\mathbf{y} \phi_j^*(\mathbf{y}) \phi_j(\mathbf{y}) V(\mathbf{x}; \mathbf{y}) \phi_i(\mathbf{x}); \\ U_{\text{eff}} &= U(\mathbf{x}) + \sum_j \int d\mathbf{y} \phi_j^*(\mathbf{y}) \phi_j(\mathbf{y}) V(\mathbf{x}; \mathbf{y}); \end{aligned} \quad (7)$$

The summations are performed over all filled orbitals. In the Restricted Hartree-Fock (RHF) method an additional constraint, $\phi_i(\mathbf{x}) = \phi_{i\#}(\mathbf{x})$, is imposed on the solutions of Eqs. (7). This provides rotational invariance of the solution. In the Unrestricted Hartree-Fock method (UHF) the additional constraint is omitted. As a result the UHF method provides much better account of electronic correlations. The price for this is a spontaneous violation of the rotational invariance.

For computations we use a finite grid. In the grid modification of the Hamiltonian (7) the kinetic energy $-\frac{\hbar^2 \nabla^2}{2m}$ is replaced by $-\frac{\hbar^2}{2m} \frac{d^2}{dn^2}$ where n is the site index of the grid. The electric current corresponding to the grid Hamiltonian reads

$$J = \frac{i\hbar}{2m} \sum_j \left(\phi_j^*(n) \frac{d}{dn} \phi_j(n+1) - \phi_j^*(n+1) \frac{d}{dn} \phi_j(n) \right); \quad (8)$$

The current is conserved because of the gauge invariance of HF equations.

For computations we use a grid of 400 points on a ring of length $L = 80$. Total z -projection of the spin is zero, so the number of electrons with spin up is equal to that with spin down, $N_\uparrow = N_\downarrow$. We perform calculations for the total number of electrons $N = N_\uparrow + N_\downarrow = 78; 118; 158$. This corresponds to the following values of the number density of electrons on the ring: $n_0 = N/L = 1; 1.5; 2$. This is the effective linear density, therefore one cannot compare n_0 quantitatively with the density of electrons in real two-dimensional leads used in experiments^{4,8}. However a qualitative comparison is possible: the smaller the real density, the smaller n_0 , and hence the smaller the Coulomb screening. Results of calculations for three different values of the barrier length, $l = 8, 10, 12$, and three different values of the electron density in the leads, $n_0 = 1, 1.5, 2$, are shown in Fig. 2. The transmission probability T is plotted versus the gate potential U_0 . Solid lines correspond to the RHF approximation.

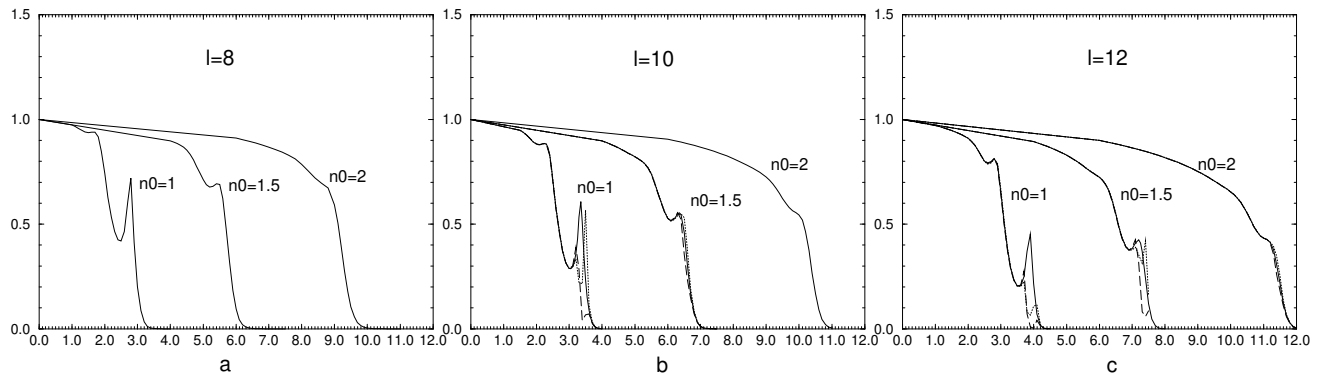


FIG. 2. Plots of the transmission probability T versus the gate potential U_0 for three different values of the barrier length, $l = 8, 10, 12$, and for three different values of the electron density in the leads, $n_0 = 1, 1.5, 2$. Solid lines show results of RHF calculations while dotted and dashed lines show spin up (T_\uparrow) and spin down (T_\downarrow) transmission probabilities calculated within the UHF method. Dotted and dashed lines in Fig. "a" ($l = 8$) are not distinguishable from solid ones.

The RHF calculation for $n_0 = 2$ has been performed earlier in Ref.⁷. All the plots presented in Fig. 2 clearly demonstrate structures of the conductance. An important point is that reduction of the electron density in leads and hence reduction of screening results in enhancement of the structure. Another feature is the evolution of the

structure down for longer contacts. The results of UHF calculations are shown in the same Fig.1 by dotted and dashed lines. The dotted line shows the transmission probability for the spin "up" channel and the dashed line shows the same for the spin "down" channel. Certainly the choice of "up" and "down" is arbitrary, one can swap the spins. The UHF method always gives two degenerate solutions. For $l=8$ the UHF results are not presented because they are hardly distinguishable from that of the RHF method shown by solid lines. According to Eq. (2) the observable transmission coefficient is the average of T_{\uparrow} and T_{\downarrow} . The results of RHF and UHF methods are very close. To demonstrate the closeness we also present in Fig.3 plots of electron densities $n_{\uparrow}(x)$ and $n_{\downarrow}(x)$ for parameters $(U_0 = 6.1, n_0 = 1.5)$ and $(U_0 = 6.4, n_0 = 1.5)$ that correspond to two points on the shoulder in Fig.2b. Solid lines represent the RHF density, $n_{\uparrow}(x) = n_{\downarrow}(x)$. The dotted line and the dashed line represent UHF densities $n_{\uparrow}(x)$ and $n_{\downarrow}(x)$ correspondingly. In case (a) $(U_0 = 6.1, n_0 = 1.5)$ the dotted and the dashed lines are not distinguishable from the solid one. In case (b) $(U_0 = 6.4, n_0 = 1.5)$ they are distinguishable, but very close.

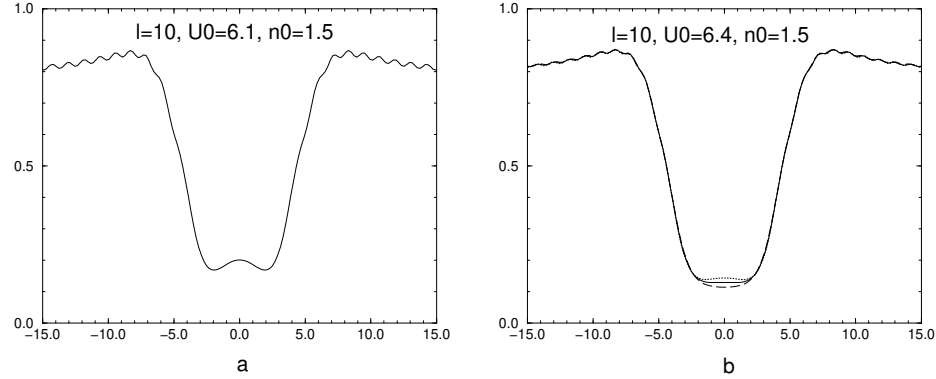


FIG. 3. Electron densities $n_{\uparrow}(x)$ and $n_{\downarrow}(x)$ for parameters $(U_0 = 6.1, n_0 = 1.5)$ and $(U_0 = 6.4, n_0 = 1.5)$ that correspond to two points on the shoulder in Fig.2b. The solid lines show RHF density, $n_{\uparrow}(x) = n_{\downarrow}(x)$. The dotted line and the dashed line show UHF densities $n_{\uparrow}(x)$ and $n_{\downarrow}(x)$ correspondingly. In the case (a), $(U_0 = 6.1, n_0 = 1.5)$, the dotted and the dashed lines are not distinguishable from the solid one.

According to Fig.2 the RHF and UHF methods really disagree only at $l=12, n_0=1, U_0 > 3.7$: relatively long contact, very low electron density in leads, and small conductance. This is the regime where the Kondo model is relevant. To understand what is going on in this situation we present in Fig.4 plots of electron densities $n_{\uparrow}(x)$ and $n_{\downarrow}(x)$ at $U_0 = 4$. As in the above figures, the solid line represents the RHF calculation, and dotted and dashed lines represent the UHF calculation.

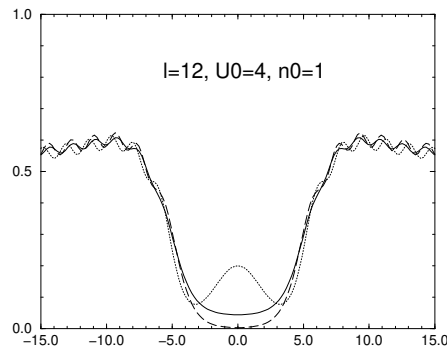


FIG. 4. Electron densities for parameters $l=12, n_0=1$, and $U_0=4$ that correspond to the structure in the left curve in Fig.2c. The solid line shows the RHF density, $n_{\uparrow}(x) = n_{\downarrow}(x)$. The dotted line and the dashed line show UHF densities $n_{\uparrow}(x)$ and $n_{\downarrow}(x)$ correspondingly.

Clearly in this situation the RHF approximation is wrong. According to the UHF calculation the spin down electron density within the contact is practically zero and, on the other hand, there is one spin up electron localized in the contact. There is no doubt that in this case dynamics of the contact is Kondo-like. In this case even the UHF method does not give a correct transmission coefficient because the method does not take into account long-range Kondo dynamics. However, fortunately, the answer is well known; the transmission coefficient is peaked up to unity, see Ref.²⁰. So, the correct plot of the transmission coefficient at $l=12$ and $n_0=1$ coincides with that presented in Fig.2c for $U_0 < 3.7$, and then there is a narrow peak up to $T=1$ at $U_0=4$. It is interesting to note that the transmission coefficients calculated within the Hartree-Fock approximation for $n_0=1$ and for shorter contacts (Fig.2a,b) have a qualitatively similar dependence: deep minimum and a narrow peak. This similarity

clearly demonstrates how the several-electron bound state that can be assessed by the Hartree-Fock method (Fig 2a, $n_0 = 1$) evolves to the multi-electron Kondo bound state that cannot be assessed by this method (Fig 2c, $n_0 = 1$).

It is interesting that for longer contacts one can trap more than one electron in the contact. To illustrate this in Fig.5 we show UHF electron densities $n_+(x)$ and $n_-(x)$ for a contact of length $l = 20$ and density in the leads $n_0 = 0.56$. In this case the two electron solution of the type shown in Fig.5a is realized at the gate potential $1.3 < U_0 < 1.85$, then at $1.85 < U_0 < 2.15$ the solution "jumps" to the single electron state shown in Fig.5b. At the higher gate potential there are no electrons in the contact. So adjusting the length of the contact, the density of electrons in leads, and the gate potential one can pin within the contact a single electron like it is shown in Fig.4 and Fig.5b or even the two electron "molecule" shown in Fig.5a. However, before getting to this very strongly correlated regime the transmission probability dips down to the value of few percent. At most the probability in the dip is 20% as it is shown in Fig.2c ($n_0 = 1$). There are no such dips in experimental data. Therefore it is unlikely that Kondo dynamics can be relevant to the effects observed in works^{4,8}. On the other hand the plots shown in Figs.2a,b,c for $n_0 = 1.5$ and $n_0 = 2$ look very similar to the experimental data. Structures on these plots are related to the few-electron spin dependent bound state. The closest physical analogy in this case is probably the Peierls spin-density instability.

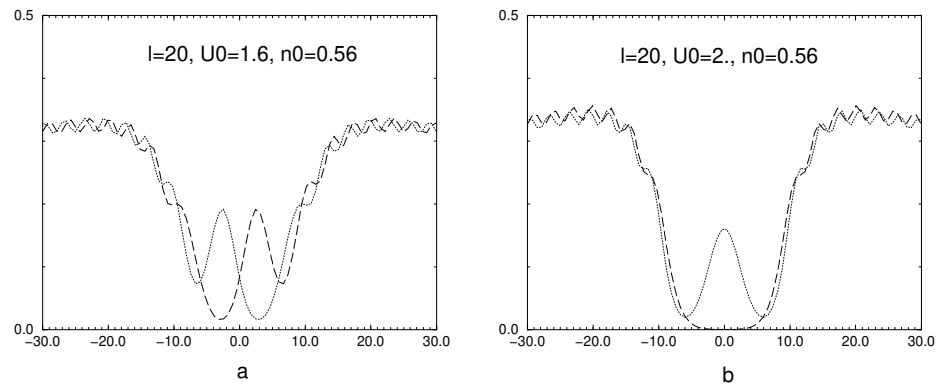


FIG. 5. UHF electron densities $n_+(x)$ (dotted line) and $n_-(x)$ (dashed line) for a "very" long contact, $l = 20$, and for a "very" low electron density in leads, $n_0 = 0.56$.

In conclusion, within a one-dimensional model we have analyzed the conductance of a short quantum contact at zero temperature. Restricted (RHF) and unrestricted (UHF) Hartree-Fock methods have been used in the analysis. Both methods clearly demonstrate structures very similar to that observed in Refs.^{4,8}. Agreement between RHF and UHF methods confirms the validity of both approximations. The conductance structure is related to the charge density wave developed in the contact. This is a spin dependent effect because without the exchange interaction the structure disappears, so this is a kind of spin-dependent bound state within the contact. Reduction of the electron density in the leads and hence reduction of the screening results in enhancement of the structure. The structure evolves down for longer contacts.

Having the contact long enough, the density of electrons in the leads low enough, and adjusting the gate potential one can pin within the contact a single electron or even a two electron "molecule". The single electron would imply Kondo-like dynamics as has been suggested in Refs.^{8,18}. However, according to our calculations, before getting to this regime the transmission probability as a function of the gate voltage dips down to at least 20%. Such dip has never been observed experimentally. Therefore it is unlikely that Kondo dynamics can be relevant to the effects observed in works^{4,8}.

I am grateful to P. G. Silvestrov for very helpful discussions. The work has been started at the Institute for Theoretical Physics at the University of California Santa Barbara, supported by the National Science Foundation under Grant No. PHY 99-07949. The work has been completed at INT at the University of Washington, supported DOE Grant DE-FG 03-00ER 41132. I acknowledge both institutes for hospitality and support.

¹ D. A. Wharam, T. J. Thornton, R. Newbury, M. Pepper, H. Ritchie, G. A. C. Jones, J. Phys. C 21, L209 (1988).

² B. J. van Wees, H. van Houten, C. W. J. Beenakker, J. G. Williamson, L. P. Kouwenhoven, D. van der Marel, C. T. Foxon, Phys. Rev. Lett. 60, 848 (1988).

³ R. Landauer, Z. Phys. 68, 217 (1987). M. Buttiker, Phys. Rev. B 41, 7906 (1990).

- ⁴ K. J. Thomas, J. T. Nicholls, M. Y. Simmons, M. Pepper, D. R. Mace, and D. A. Ritchie, Phys. Rev. Lett. 77, 135 (1996).
- ⁵ K. J. Thomas, J. T. Nicholls, N. J. Appleyard, M. Y. Simmons, M. Pepper, D. R. Mace, W. R. Tribe, and D. A. Ritchie, Phys. Rev. B 58, 4846 (1998).
- ⁶ A. Kristensen, H. Bruus, A. E. Hansen, J. B. Jensen, P. E. Lindelof, C. J. Marckmann, J. Nygard, C. B. Sorensen, F. Beuscher, A. Forchel, and M. Michel, Phys. Rev. B 62, 10950 (2000).
- ⁷ D. J. Reilly, G. R. Facer, A. S. Dzurak, B. E. Kane, R. G. Clark, P. J. Stiles, J. L. O'Brien, N. E. Lumpkin, L. N. Pfeiffer, and K. W. West, Phys. Rev. B 63, 121311 (2001).
- ⁸ S. M. Cronenwett, H. J. Lynch, D. G.oldhaber-Gordon, L. P. Kouwenhoven, C. M. Marcus, K. Hirose, N. S. Wingreen, V. Umansky, Phys. Rev. Lett. 88, 226805 (2002).
- ⁹ Chuan-Kui Wang and K.-F. Berggren, Phys. Rev. B 54, 14257 (1996); Phys. Rev. B 57, 4552 (1998).
- ¹⁰ L. Camels and A. Gold, Solid State Commun. 106, 139 (1998).
- ¹¹ N. Zabala, M. J. Puskas, and R. M. Nieminen, Phys. Rev. Lett. 80, 3336 (1998).
- ¹² B. Spivak and F. Zhou, Phys. Rev. B 61, 16730 (2000).
- ¹³ A. M. Bychkov, I. I. Yakimenko, and K.-F. Berggren, Nanotechnology 11, 318 (2000).
- ¹⁴ V. V. Flambaum and M. Yu. Kuchiev, Phys. Rev. B 61, R7869 (2000).
- ¹⁵ T. Rejec, A. Ramak, and J. H. Jefferson, Phys. Rev. B 62, 12985 (2000).
- ¹⁶ E. Lieb and D. Mattis, Phys. Rev. B 125, 164 (1962).
- ¹⁷ O. P. Sushkov, Phys. Rev. B 64, 155319 (2001).
- ¹⁸ Y. M. eir, K. Hirose, and N. S. Wingreen, cond-mat/0207044.
- ¹⁹ R. A. Molina, D. Weinmann, R. A. Jalabert, G.-L. Ingold, and J.-L. Pichard, cond-mat/0209552.
- ²⁰ L. I. Glazman and M. E. Raikh, Pis'ma Zh. Eksp. Teor. Fiz. 47, 378 (1988) [JETP Lett. 47, 452 (1988)]; T. K. Ng and P. A. Lee, Phys. Rev. Lett. 61, 1768 (1988); N. S. Wingreen and Y. M. eir, Phys. Rev. B 49, 11040 (1994).